CHAPTER – II

THEORETICAL BACKGROUN

2.1 INTRODUCTION

The materials in the form of the films are widely used in optoelectronic devices, photoelectrochemical devices, thermoelectric coolers, electrical switching, solar selective and decorative coatings etc. The utility and performance of semiconductor devices depends critically on the properties of the semiconductor materials. So it is necessary to study the basic characterization of the material in order to asses the scope for further improvements in the utility and efficiency.

The present chapter, therefore, focuses on the theoretical aspects of various characterization techniques used for studying the properties of thin film materials. X–ray diffraction (XRD), Scanning Electron Microscopy (SEM), Electrical resistivity, Thermoelectric power (TEP), Optical absorption, Photoelectrochemical characterization techniques and the various aspects concerning Semiconductor–Septum storage cell have been discussed in the next sections.

2.2 THIN FILM THICKNESS

The film thickness, being one of the important parameters which affects the properties of the film, is measured in present investigation by weight difference method called as gravimetric method. Suppose ‘m’ is a mass of the thin film deposited on the substrates which covers the area ‘A’ cm^2, the thickness ‘t’ is calculated by using known mass ‘m’ and density ‘ρ’ of the

material. The value pertaining to the bulk material is usually taken for ‘ρ’ even when the actual density of the thin film is lower. The thickness is calculated from the relation [1].

$$t = m / A.\ \rho \qquad (2.1)$$

The mass ‘m’ of the film deposited can be measured by using one pan semimicrobalance.

2.3 X–RAY DIFFRACTION (XRD) TECHNIQUE

A given substance always produces a characteristic diffraction pattern, whether that substance is present in the pure state or as one constituent of a mixture of substances. This fact is the basis for the diffraction method of chemical analysis. Qualitative analysis for a particular substance is accomplished by identification of the pattern of that substance. Quantitative analysis is also possible, because the intensities of the diffraction lines due to one phase of a mixture depend on the proportion of that phase in the specimen.

Detailed treatments of chemical analysis by X–ray diffraction are given by Klug and Alexander [2] and Zwell and Danko [3]. Nenadic and Crable [4] have reviewed diffraction methods of determinig quartz, asbestos and tale in industrial dust; all of these minarals can cause lung disease.

2.3.1 Basic principle of X– ray diffraction technique

The crystallographic features are studied by the process of X– ray diffraction. The X–ray technique based on monochromatic radiation is

generally more important because the spacing of the planes (d–spacing) can be deduced from the observed diffraction angles. The phenomenon of X–ray diffraction can be considered as a reflection of X–rays from the crystallographic planes of the material and is governed by Bragg's equation.

$$2\,d \sin\theta = n\lambda \qquad (2.2)$$

Where '*d*' is the lattice spacing, λ is the wavelength of monochromatic X–rays, n is the order of diffraction and θ is the diffraction angle.

For thin films, the powder technique in conjuction with diffractometer is most commonly used. In this instrument the diffracted radiation is detected by the counter tube which moves along the angular range of reflections. The intensities are recorded on a computer system. The '*d*' values are calculated using relation 2.2 for known values of θ, λ and n. The X–ray diffraction data thus obtained is printed in tabular form on paper and is compared with Joint Committee powder Diffraction Standards (JCPDS) data to identify the unknown material. Typical JCPDS data card of sodium chloride is shown in Fig. 2.1. The X–ray diffraction data can also be used to determine the dimensions of the unit cell.

2.4 SCANNING ELECTRON MICROSCOPY (SEM)

The SEM is used primarily for the examination of thick (i.e. electron opaque) samples. Electrons which are emitted or back scattered from the specimen are collected to provide :

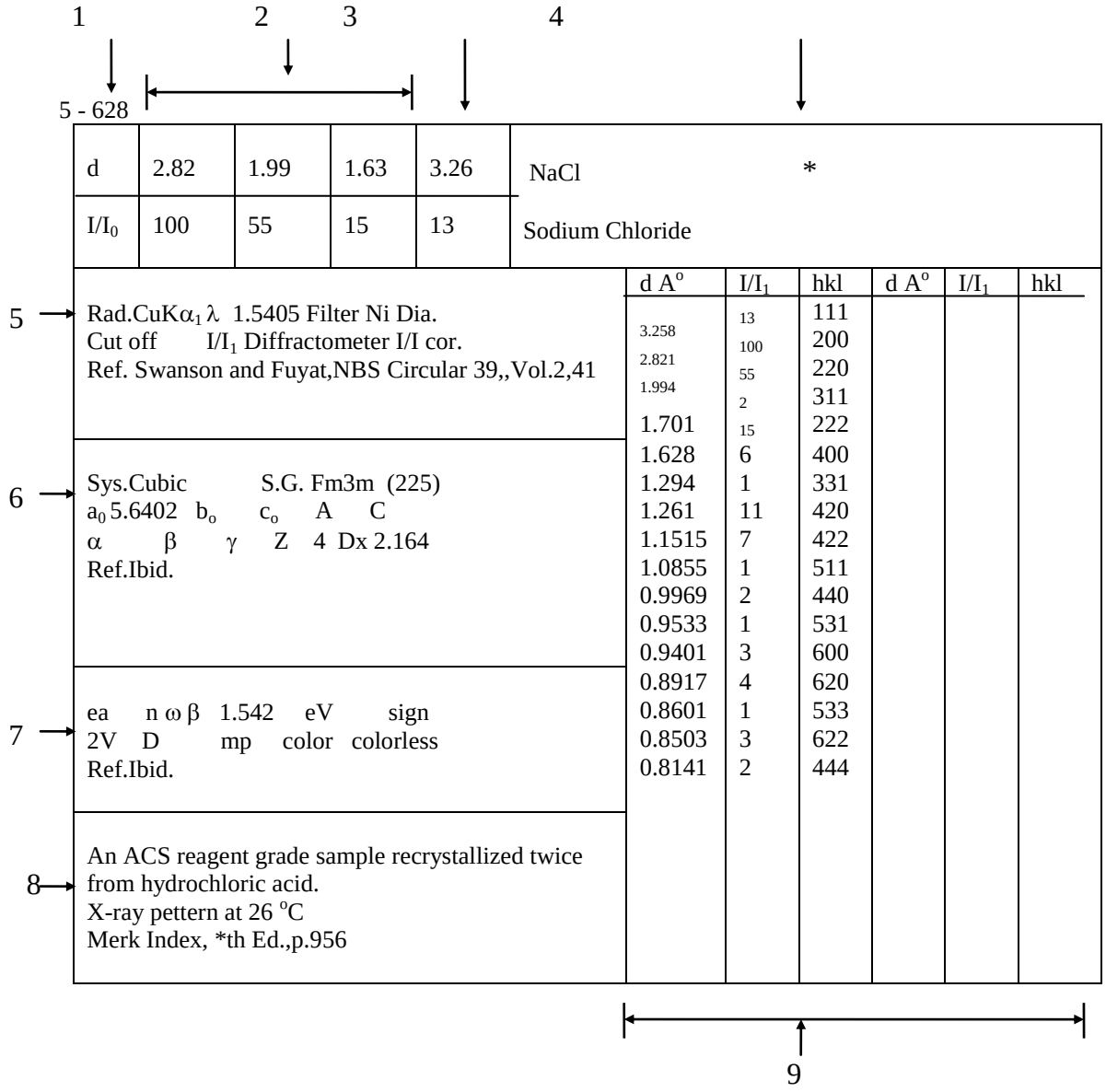

Fig. 2.1: Typical JCPDS diffraction data card for sodium chloride. Appearing on the card are 1 (file number), 2 (three strongest lines), 3 (lowest single line), 4 (chemical formula & name of the substance), 5 (data on diffraction method used), 6 (crystallographic data), 7 (optical and other data), 8 (data on specimen), 9 (diffraction pattern). Intensities are expressed as percentage of I_1, the intensities of the strongest line on the pattern. Most cards have a symbol in the upper right corner indicating the quality of the data: * (high quality),I (lines indexed, intensities fairly reliable), c (calculated pattern), and o (low reliability.) (Courtesy of Joint Committee on Powder Diffraction Standards.)

(1) topological information (i.e. detailed shape of specimen surface) if the low energy secondary electrons (≤ 50 eV) are collected, (2) atomic number or orientation information if the high energy back scattered electrons are used or if the leakage current to earth is used. Imaging of magnetic samples using secondary and or back scattered electrons reveals magnetic domain contrast. In addition, two other signals can be collected, the electron beam induced current and light catholuminescence.

SEM operates generally in the range 2.5 to 5.0 eV with probe size available at the specimen between 5 nm to 2 μm. The convergence angle of the probe at the specimen is controlled by the diameter of the final aperture and this angle determines the depth of field of an SEM. Thus the large depth of field F which is commonly associated with SEM images is in fact due to small convergence angle at the specimen, which is much smaller than the corresponding angle in optical microscopes. A very large value of depth of field for high resolution image which underlines the value of high magnification SEM images of rough surfaces.

2.5 TRANSPORT PROPERTIES

Surface transport phenomena are well known to have a strong influence on the electronic properties of bulk semiconductors. These phenomena play an important role in the transport properties of semiconducting film of about 1 μm thickness and having carrier concentration upto 10^{18} cm^{-3}. This role results

from the fact that when transport takes place through thin specimen, the carriers are subjected to considerable scattering by the boundary surface in addition to normal bulk scattering. This additional scattering will reduce the effective carrier mobility below the bulk value and will thus give rise to conductivity size effects. A study of these size effects can yield information on the electronic structure of a surface and is therefore of fundamental and practical importance. Surface transport phenomena in bulk semiconductors has received much attention in recent years. An excellent review of the subject is given by Pulliam et al. [5]. The important transport properties i.e. electrical resistivity and thermoelectric power are discussed in next sections.

2.5.1 Electrical Resistivity

The use of thin films as resistors, contacts and interconnections has lead to extensive study of conductivity, its temperature dependence, the effect of thermal processing stability and so on. Investigations of the electrical resistivity as a highly structure sensitive properties make it possible to gain insight into the structural and electrical properties of the metal film which is important from both the theoretical and practical point of view.

The contact technique are almost widely used for the measurements of resistivity. These techniques include two−point probe, four−point probe and the spreading resistance methods. The two−point method is simple and easy to use. In this technique a constant d.c. voltage V is applied between two fixed position probes of separation d and a current I passing through the samples of

known dimensions (cross section area ‘A’) is measured with an appropriate current meter. For uniform sample, resistivity is given by,

$$\rho = (A/I)\,(V/d) \qquad (2.3)$$

In case of semiconducting thin films, the resistivity decreases with increase in temperature. The thermal activation energy E_a is calculated by using conductivity relation [6]

$$\sigma = \sigma_o \exp(-E_a / KT) \qquad (2.4)$$

where symbols have their usual meanings. The slope of the log (σ) versus (1/T) leads to the estimation of activation energy.

2.5.2 Thermoelectric power (TEP)

It is well known that if a metal is connected at its two ends with a second metal and if one of the junction is heated, a voltage is developed across the open ends of the second metal. If some metal contacts are applied to the two ends of a semiconductor rod or thin film and if one junction is maintained at higher temperature than the other, a potential difference is developed between the two electrodes. This thermoelectric or Seebeck voltage is produced partly because : 1) The majority carriers in the semiconductor diffuse from hot to cold junction, thus giving a potential difference between the ends of the specimen. This voltage builds upto a value such that the return currents just balances the diffusion current when a steady state is reached. 2) Other part which contributes to the thermoelectric voltage is the contact potential difference between metal and semiconductor which occurs at two junctions.

In a semiconductor, if the charge carriers are predominately electrons, the cold junction becomes negatively charged and if the charge carriers are positive holes, the cold junction becomes positively charged. The magnitude of the developed voltage is proportional to the difference in temperature between the hot and the cold junction, if the temperature is small. From the sign of the thermoelectric voltage it is thus possible to deduce whether a given specimen exhibits *n*– or *p*– type conductivity.

The thermoelectric power (TEP) which is defined as the ratio of thermally generated voltage to the temperature difference across the semiconductor, gives the information about the type of carriers in the semiconductors. TEP is used to evaluate carrier mobility and carrier concentration using relation.

$$TEP = K\, e \{ A + Ln [2 (2 \pi me^* KT)^{3/2}]\} \quad (2.5)$$

Where A is the thermoelectric factor. Other symbols have their usual meanings. After substituting the various constants equation (2.5) simplifies to [7]

$$\log (n) = (3/2) \log (T) - 0.005\, TEP + 15.719 \quad (2.6)$$

The mobility μ of the charge carriers is determined from the relation

$$\mu = \sigma / ne \quad (2.7)$$

where n is the electron density and σ is the conductivity.

2.5.3 Optical absorption

The equilibrium situation in semiconductor can be disturbed by generation of carriers due to optical photon absorption. Optical photon incident

on any material may either be reflected, transmitted or absorbed. The phenomena of radiation absorption in a material is altogether considered to be due to 1) inner shell electrons, 2) valence band electrons, 3) free carriers including as well as electrons and 4) electrons bound to localized impurity centers or defects of some type. In study of fundamental properties of the semiconductors, the absorption by the second type of electrons is of great importance. In an ideal semiconductor, at absolute zero temperature the valence band would be completely full of electrons, so that electron could not be excited to higher energy state from the valence band. Absorption of quanta of sufficient energy tend to transfer of electrons from valence band to conduction band.

The optical absorption spectra of semiconductors generally exhibits a sharp rise at a certain value of the incident photon energy which can be attributed to the excitation of electrons from the valence band to conduction band (may also involve acceptor or donor impurity levels, traps, excitons etc.) The conservation of energy and momentum must be satisfied in optical absorption process.

Basically there are two types of optical transitions that can occur at the fundamental edge of the crystalline semiconductor, direct and indirect. Both involve the interaction of an electromagnetic wave with an electron in the valence band, which is rose across the fundamental gap to the conduction band. However, indirect transition also involve simultaneous interaction with lattice vibration. Thus the wave vector of the electron can change in the optical

transition. The momentum change being taken or given up by phonon. Direct interband optical transition involves a vertical transition of electrons from, the valence band to the conduction band such that there is no change in the momentum of the electrons and energy is conserved as shown in Fig. 2.2 (a). The optical transition is denoted by a vertical upward arrow. The forms of the absorption coefficient α as a function of photon energy $h\nu$ depend on the dependence on energy of N(E) for the bands containing the initial and final states. For simple parabolic bands and for direct transitions [8].

$$\alpha = A (h\nu - Eg)^n / h\nu \qquad (2.8)$$

Where A is a constant depending upon the transition probability for direct transition, n=1/2 or 3/2 depending on whether the transition is allowed or forbidden in the quantum mechanical sense. Eg is the optical gap.

Lets visualize a situation given in Fig. 2.2 (b) where interband transition takes place between different k– states. Since these must satisfy the momentum conservation laws, the only way such transition can take place is through the emission or absorption of a phonon with wave vector q i.e.

$$k' \pm q = k + K \qquad (2.9)$$

The transitions defined by equation (2.9) are termed indirect transitions. For indirect transitions [9]

$$\alpha = A (h\nu - Eg)^n / h\nu \qquad (2.10)$$

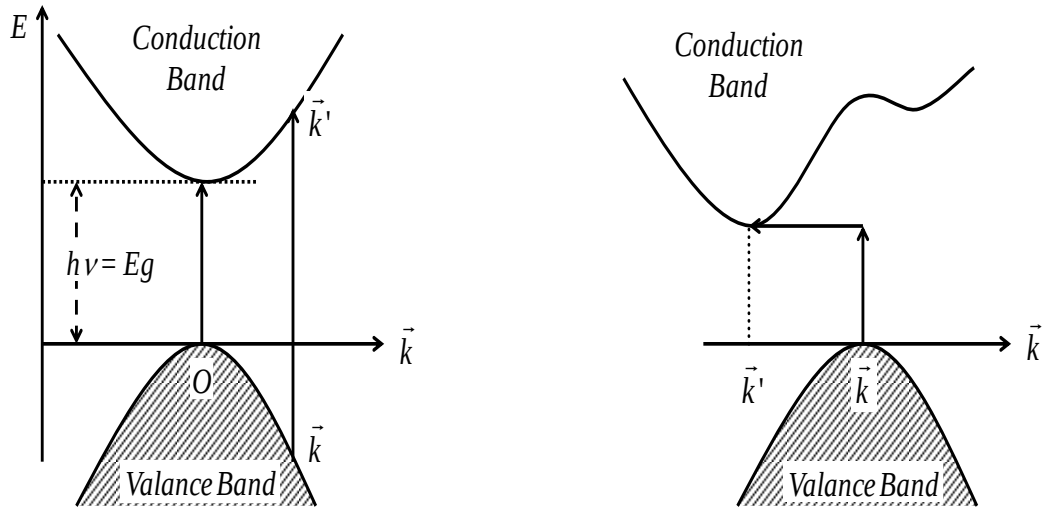

Fig.2.2- "Direct interband optical transitions" for (a) direct band and (b) indirect band semiconductors. The transitions are represented by vertical arrows.

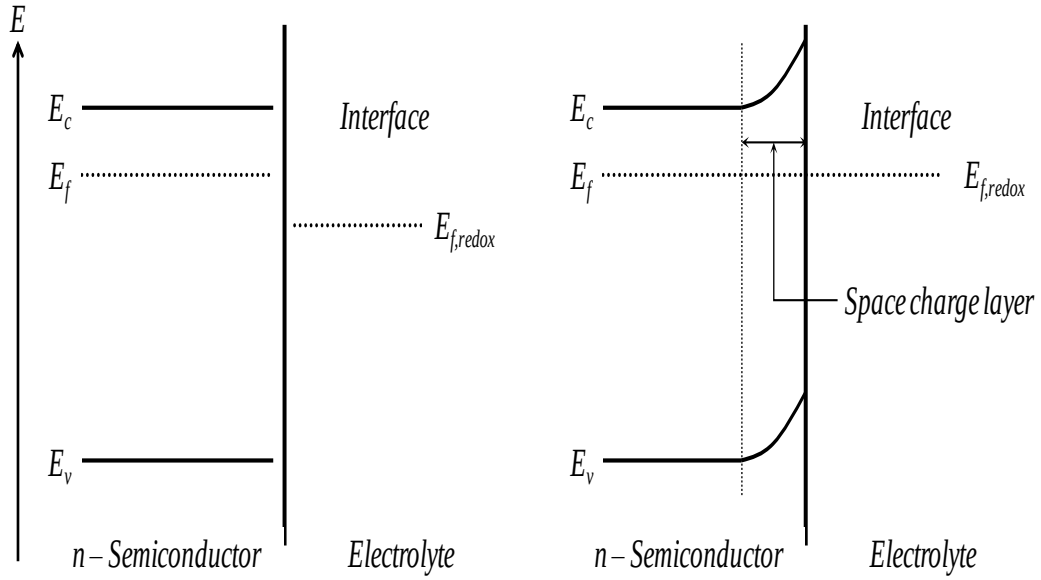

Fig. 2.3- Band bending at n-type semiconductor-electrolyte interface a) before contact and b) after contact and equilibrim of Fermi levels

For allowed transition n=2 and for forbidden transitions n=3.

The band gap energy ‘Eg’ is determined by extrapolating the linear portion of the plot of $(\alpha h\nu)^n$ against $h\nu$ to the energy axis at $\alpha = 0$.

While discussing the optical absorption edges observed in amorphous semiconductors the following assumptions are made : (a) The matrix elements for the electronic transitions are constant over the range of photon energies of interest. (b) K– conservation selection rule is relaxed. This assumption is made in amorphous semiconductors because, near the band edges at least, $\Delta k \sim k$ and thus k is not a good quantum number. On E – k diagram such transitions would be non–vertical. However, no phonon absorption or emission processes are invoked to conserve momentum and all the energy required is provided by the incident photons. Such transitions are termed non–direct as opposed to indirect.

Without knowledge of the form of N(E) at the band edges, and under the assumption of parabolic bands, the absorption in many amorphous material is observed to obey the relation (2.8) with n=2. Thus absorption edge of many amorphous semiconductors can be described by a simple power law, at least over a limited range of the absorption coefficients, which enables an optical gap Eg to be defined.

2.6 PHOTOELECTROCHEMICAL (PEC) SOLAR CELL

There are several methods of collecting and converting solar energy viz. photovoltaic, photoelectrochemical, photothermal and photosynthetic. Out of these routs the photoelectrochemical system is easiest one. The photovoltaic effect was first reported in 1839 by Becquerel [9]. A PEC effect is defined as one in which irradiation of electrode / electrolyte system produce a change in electric potential (on open circuit) or in the current flowing in external circuit (under short circuit conditions)[10].

Semiconductor / liquid junction cells have several advantages over solid state junction cells which make them attractive. Simple immersion of the semiconductor into the liquid forms the junction. Another desirable feature is that the electron–hole pairs are created in a region of high field, producing efficient charge separation (in a photovoltaic device charge generation occurs in solution far way from the electrode, resulting in poor quantum efficiency). Direct gap materials are potentially used as the photoelectrode. There is no front contact on the photoelectrode and there may be no need for an antireflection coating. The possible generation of fuels is viewed as an advantage, and a third electrode can be used as a storage electrode to allow the PEC cell to be used as a photochargeable battery.

2.6.1 Semiconductor electrolyte interface

When an electrode is dipped into an electrolyte, the excess charge residing on the electrode surface must be exactly balanced by an equal charge

of opposite sign on the solution side. This can happen by charge transfer across the electrode–electrolyte system [11-12].

2.6.2 Space charge region in the semiconductor

Fig 2.3 shows the energy band diagram for n–type semiconductor and an electrolyte (a) before and (b) after establishing the contact between them. Fermi levels, $E_{f,semi}$ and $E_{f,redox}$ are at different levels resulting in electron transfer from semiconductor to electrolyte which establishes the equilibrium. This flow of electrons results in the accumulation of ions in the semiconductors to form the space charge region near the interface in the semiconductor. A strong local electric field is developed and band bending takes place.

The potential drop in the semiconductor space charge layer depends on the difference between the Fermi levels of semiconductor and the redox electrolyte, if the former is free from excess charge.

2.6.3 Helmholtz double layer

The Helmholtz layer is formed on the solution side. When only electrostatic interaction operates, ions from the solution side may approach the electrode only so far as their inner solvation cells will allow. The surface array of ions is thus ‘cushioned’ from the electrode surface by a layer of solvent molecules. The line drawn through the center of such ions at the distance of closest approach makes the boundary known as outer Helmholtz plane. The region within this plane constitutes the compact part of the double layer or Helmholtz layer.

In other cases, specific absorption of ions may occur where va*n*-der-waals and chemical forces participate. Most anions are specifically adsorbed, thereby loosing most of their inner hydration shell, but most cations retain their hydration molecules. Specially adsorbed species can approach much closer to the electrode surface. A line drawn through the centers of such species aligned at the electrode surface defines a further boundary within the Helmholtz layer, the so-called inner Helmholtz layer plane. The extent to which the specific adsorption occurs is controlled by the nature of the ions in the solution as well as the nature of the electrode material and the potential applied to it. The relative position of the inner and outer Helmholtz planes of the electrode double layer [13] are shown in Fig. 2.4.

Uncharged species, if they are less polar than the solvent or are attached to the electrode material by va*n*-der-waals or chemical forces, will accumulate at the interface such species are known as surfactants, when specific adsorption occurs, the charge distribution in the diffusion layer will change to maintain the electroneutrality.

2.6.4 Gouy–Chapman (diffuse) layer

The size of the ions forming the outer Helmholtz plane is such that the sufficient number of them can not neutralize the charge on the electrode. Therefore the remaining charges are held with increasing disorder as the distance from the electrode surface increases and electrostatic forces become weaker and dispersion by thermal motion is more effective. This less ordered charges forcing opposite to that on the electrode constitutes the diffuse part of

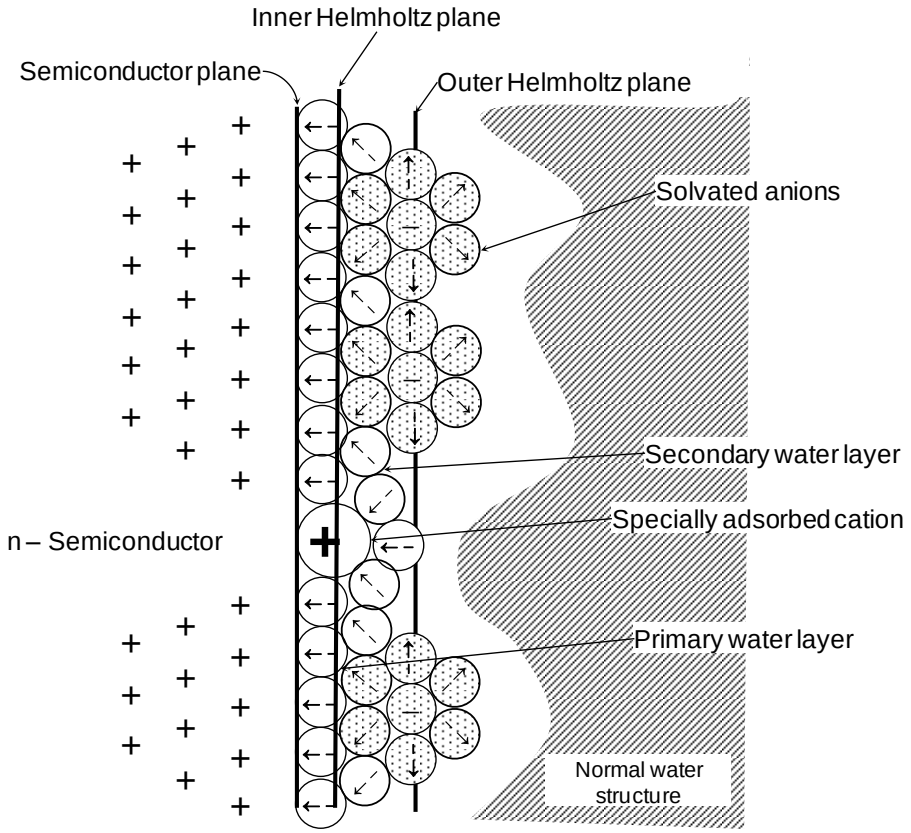

Fig. 2.4 – Relative positions of inner and outer Helmholtz electrode double layer

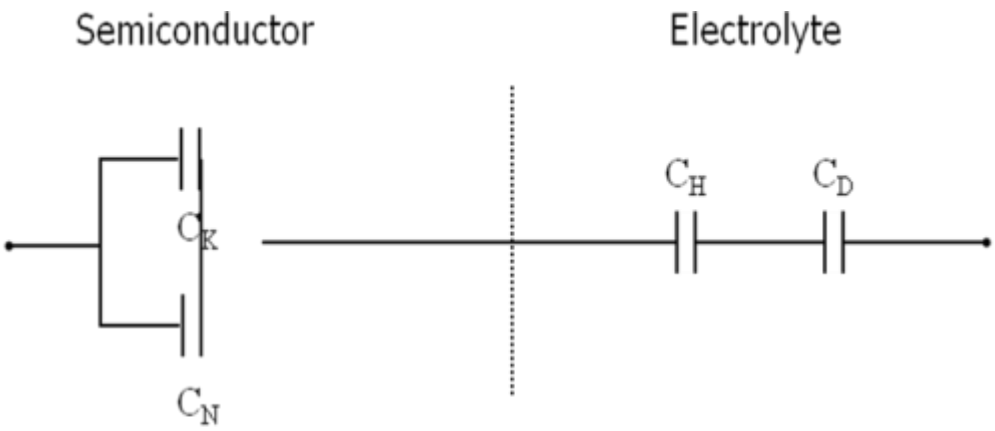

Fig. 2.5 – Equivalent circuit diagram of capacitance formed at semiconductor – electrolyte interface.

the double layer. Thus all the charge which neutralize that on the electrode is held in a region between the outer Helmholtz plane and the bulk of electrolyte solution. The additional charges required to neutralize the total charge on electrode forms the Gouy–Chapman layer.

The total capacitance of the double layer is made up to that due to the inner (adsorption) layer C_H and that due to the diffuse layer C_D, since these two capacitances are connected in series, the equivalent capacitance is [11, 14 -15]

$$(1 / C) = (1 / C_H) + (1 / C_D) \qquad (2.11)$$

The series capacitance of semiconductor–electrolyte junction is shown in Fig. 2.5.

2.6.5 Stern Model

Stern (1944) presented a synthesis of the Helmholtz and Gouy–Chapman model of the double layer. Stern theory suggests that the ions, being of finite size, keep a minimum distance of approach of the electrode surface. Thus, The electrolyte side of the double layer is neither abrupt nor diffuse but a combination of the two. In this situation the electrolyte side of the interface is divided into two regions. 1) A dense layer of ions stuck to the electrode: In this region the potential varies linearly with distance. 2) A diffused layer of ions: This is formed as a result of opposing tendencies of the attractive Couloumbic force and disordering thermal fluctuations. The potential decays exponentially. The Stern model does not tell explicitly how the ions are stuck to the electrode.

For a semiconductor, the charge transfer results in a space charge region in the semiconductor and Helmholtz double layer and Gouy–Chapman diffuse layer in the electrolyte as shown in the Fig. 2.6.

2.6.6 Photoinduced charge transfer across semiconductor electrolyte junction

The region of the photopotential can now be understood by considering the changes that occur at such an interface by the absorption of band gap radiation. Irradiation of the semiconductor electrolyte interface produce electron–hole pairs, the electrons being promoted to the conduction band. The potential difference across the space charge layer causes the electrons to move towards the bulf of the semiconductor as this is down hill path for the electrons in an n– type semiconductor. The minority carriers h^+ move towards the surface of the electrode. This movement of the charge carriers in the field of the space charge layer counteract the band bending, causing as partial return to the charge carrier distribution as before bend bending and is shown in Fig. 2.7. The result is the development of a Fermi level in the semiconductor called the photo–Fermi level which is no longer equal to the redox potential of the electrolyte $E_{f(photo)} - E_{f(redox)}$ goes up as the photopotential on illuminating the interface with light ($h\nu \geq Eg$) [16].

A photocurrent can now be observed by connecting the photoanode to a suitable counter electrode. The photocurrent depends on the absorption coefficient of the semiconductor, width of the space charge region, hole diffusion length, area of illuminated electrode, photon energy and radiation

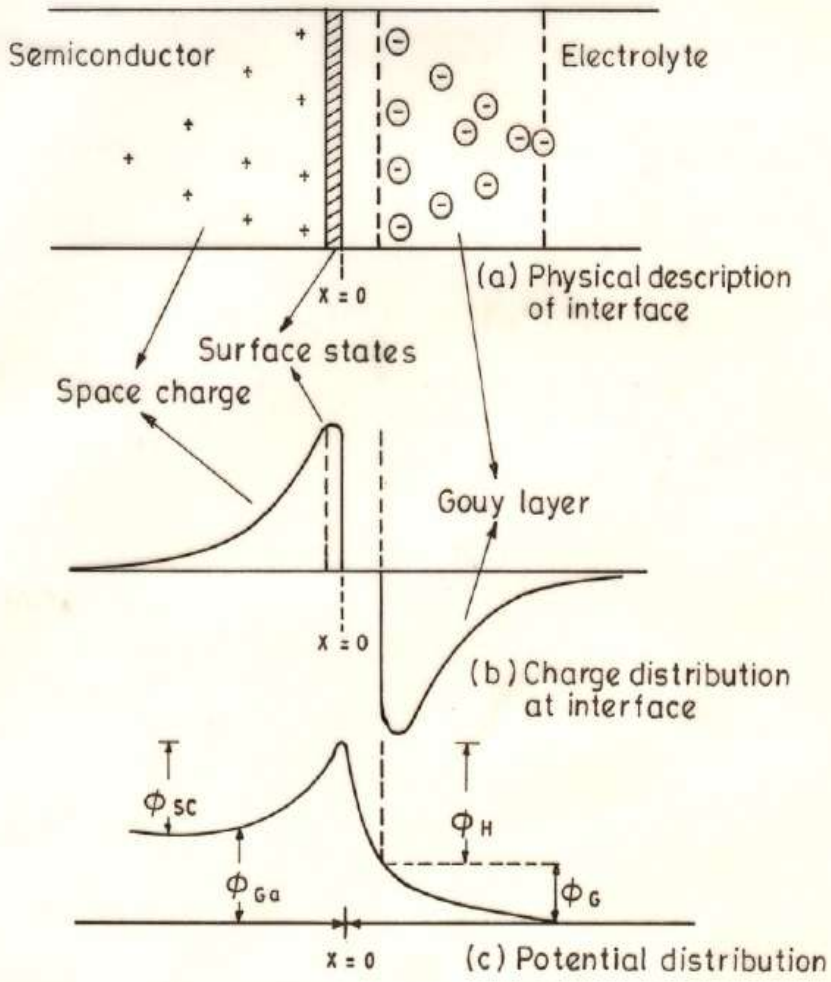

Fig. 2·6 – Charge and potential distribution at the semiconductor electrolyte interface $\Phi_{SC}, \Phi_H, \Phi_G, \Phi_{Ga}$ are respectively potentials across the space charge layer, Helmholtz layer, Gouy layer and Galvanic potential.

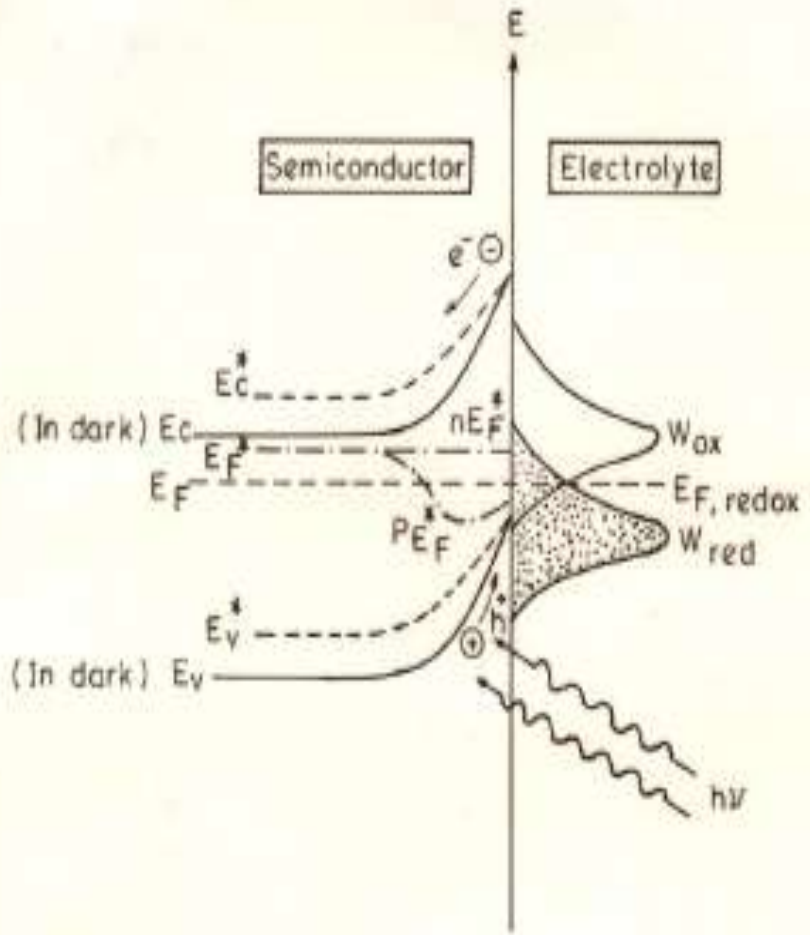

Fig. 2-7 - The position of energy bands under illumination (starred values) responsible for photoinduced charge transfer.

intensity. Under short circuit conditions, the Fermi levels of the semiconductor and the potential of the redox couple of the solution are equalized and a net charge flows during the illumination.

A typical PEC cell and energy level diagram for *n*– type semiconductor based PEC cell are shown in Fig. 2.8 (a) and (b) respectively.

2.6.7 Some efficiency considerations

A semiconductor electrode has a threshold for light absorption which is ideally by the band gap. All the light energy below threshold gets lost i.e. for activation of photovoltaic devices photons of threshold energy are required. The energy conversion efficiency (η), therefore, depends on the band gap and is given by a relation [10, 17]

$$\eta = E_{stor} \int \alpha\,(E)\, N(E)\, dE \,/\, \int E_{ther}\, N(E)\, dE \qquad (2.12)$$

Where E_{ther} is the threshold energy for light absorption. N(E) the number of photons with energy E, α(E) the fraction of photons adsorbed and E_{stor} the cell voltage. From equation (2.12) it is the expected that the efficiency is maximum if :

i) a band gap of semiconductor is high,

ii) α(E) is high, where

$$\alpha(E) = A\,(h\nu - Eg)^{n} / h\nu \qquad (2.13)$$

where n=1/2 or 2 for direct or indirect semiconductors.

In order to have high value of α(E), Eg, should be small. These conditions lead to a contradictory conclusions. Hence efficiency should be

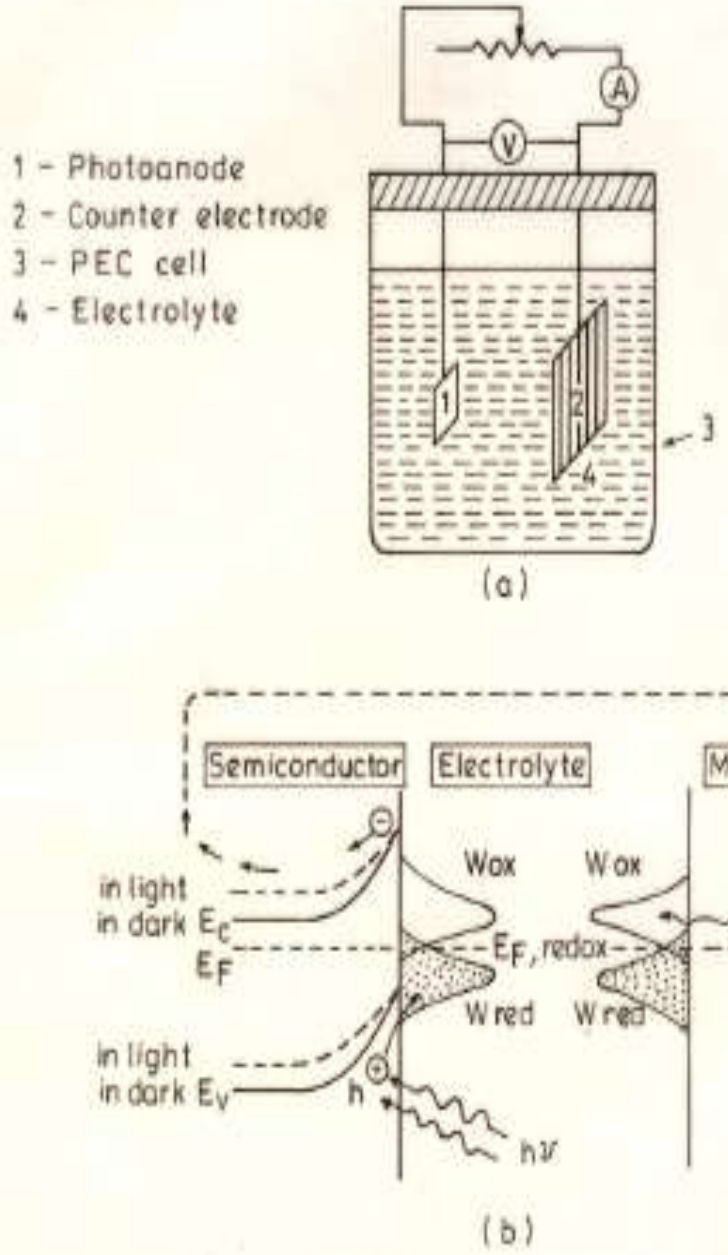

Fig. 2-8 - a) A typical electrochemical photovoltaic cell.
b) Current flow and energy level diagram for n-semiconductor PESC.

maximum at some optimum value of Eg. The energy conversion efficiency can also be expressed as [18]

$$\eta\% = \frac{\text{Maximum output power}}{\text{Input power}} \times 100 \qquad (2.14)$$

A parameter namely, fill factor (ff) is defined as

$$ff\ \% = \frac{\text{Maximum output power}}{Isc\ Voc} \times 100 \qquad (2.15)$$

where Isc and Voc are short circuit current and open circuit voltage respectively.

In addition to band gap, there are other factors which affects the efficiency of PEC cells [10] are the properties of semiconductor, energy losses due to photoinduced redox reactions, light losses due to absorption in the electrolyte, reflection from semiconductor surface, ohmic losses due to absorption in the electrolyte and semiconductor and losses due to concentration polarization.

2.7 SEMICONDUCTOR SEPTUM SOLAR CELLS

In recent years, much efforts have been directed towards developing new and better solar energy conversion / storage devices. A high degree of sophistication has already been achieved in the fabrication of p–n junction solar cells. However one of the challenging problems in solar energy research storage. Recently an alternative strategy has been suggested in which a solid–

liquid junction has been used which offers the possibility of both solar energy conversion and storage.

Recently some groups have attempted the use of a membrane based PEC system for solar energy storage devices [19-21]. The objective of most of the research carried out in this area is to optimize the efficiency and life time of these cells. Economic conditions are also important for these devices. The solar energy storage cells can be classified as

(a) Redox storage Electrode.

(b) Redox storage Electrolyte.

(c) Semiconductor septum (SC−SEP)

The first two types of redox storage cell are well known; however, the solar energy storage with the help of SC−SEP cells is promising due to its inhert properties. The origin of the SC−SEP storage cell is traceable to early studies of the membrane biophysics aspects of photosynthesis, for redox reactions. In this cell under illumination, on one side of the membrane solution interface reduction occurs while on the other side oxidation takes place. Thus the basic concept in all the systems is light induced charge separation in the form of electrons and holes which causes reduction on one side and oxidation on the other. Two different redox couples having standard potentials sufficiently wide apart from each other should be used in order to get large photovoltage. Under illumination, these chemical species can be charged and then electrochemically discharged for the production of electricity.

The SC–SEP cell can be used as an efficient storage cell if the SC–SEP electrode and electrolytes have properties listed in Table I and II respectively [22].

Table I : Semiconductor septum Electrode

SEMICONDUCTOR PHOTOELECTRODE

1. $h\nu \geq Eg$. i.e. the energy of the incident light should be greater than the band gap of the semiconductor.
2. The absorption coefficient of a semiconductor should large.
3. In order to utilize the incident light to generate electricity, the reflection and transmission coefficients must be small.
4. The local field generated after the formation of the junction should be strong enough to separate electron–hole pairs effectively.
5. Recombination states must be minimum.
6. The thickness of the bulk of the semiconductor must be optimum.

Table II : Electrolyte properties requisite for the SC– SEP cells.

	PROPERTY	ROLE
1.	Oxidation– Reduction potential	Redox reaction to be positioned appropriate to the semiconductor band edges. Electrolyte decomposition limits suitability.
2.	Electron transfer rates of Ox. and Red. species	Ideally rapid (reversible) at both semiconductor and counter electrodes suitable mass transport conditions
3.	Photo and thermal stabilities	Ox., Red. and solvent components to have

		photo and thermal stabilities throughout usable solar spectrum and operational temperature range.
4.	Surface compatibility	Non– corrosive to the electrode and containment materials. Semiconductors corrosion inhibited if necessary and undesirable surface reactions absent. e.g. absorption, dissociation, passivation etc.
5.	Optical transparency	Minimum absorption losses for solar energy spectrum
6.	Fluidity	Liquidious range and viscosity to allow convective mixing within temperature extremes
7.	Solubility	Ox., Red. and supporting electrolyte concentration in solvent or liquid matrix to be adequate to reach required current densities
8.	Conductance	Ionic conductance of electrolyte should permit negligible ohmic losses
9.	Toxicity and reactivity to environment and cost	Preferably low dependent on application

2.7.1 Energy storage with semiconductor septum cell

The concept of using SC–SEP as an energy storage is based on modeling of natural photosynthetic systems with pigmented bilayer lipid membrane [23-

26]. The chemical reactions taking place in the two compartments must be reversible, hence different metallic counter electrodes like Cd, Cu, Ag, etc. are used in electrolytic solution like $Cd(NO_3)_2$, $CuCl_2$, $Cu(NO_3)_2$, $AgNO_3$ etc. Such a cell can store energy above some threshold, the highest value of which depends on the difference between the Ef, redox potentials on the position of the band edges of the septum relative to the Fermi levels of the redox systems [22]. The schematic diagram of SC−SEP cell is shown in Fig. 2.9. Variety of semiconductors viz. CdSe, CdTe, Fe_2O_3 etc. can be used as a semiconductor septum with different electrolyte combinations,

2.7.1.1 Storage in the form of electrical energy

Semiconductor septum can be produced by using techniques like electrodeposition, coprecipitation, spray prolysis [22] etc. Different redox couples can be used in the two compartments separated by the septum. Two metallic counter electrodes are to be used in two compartments for making electrical contacts to the electrolytes. The cell contains five interfaces. If contacting electrode and electrolytes are the same in both compartments, no net chemical change takes place, because the reactions are opposite but equal. Such a cell functions merely as a transducer, changing light into electrical energy.

To achieve effective charging of the SC−SEP redox cell, it is necessary to have the redox couples (in II compartment) involving standard potentials within 500 mV negative of it.

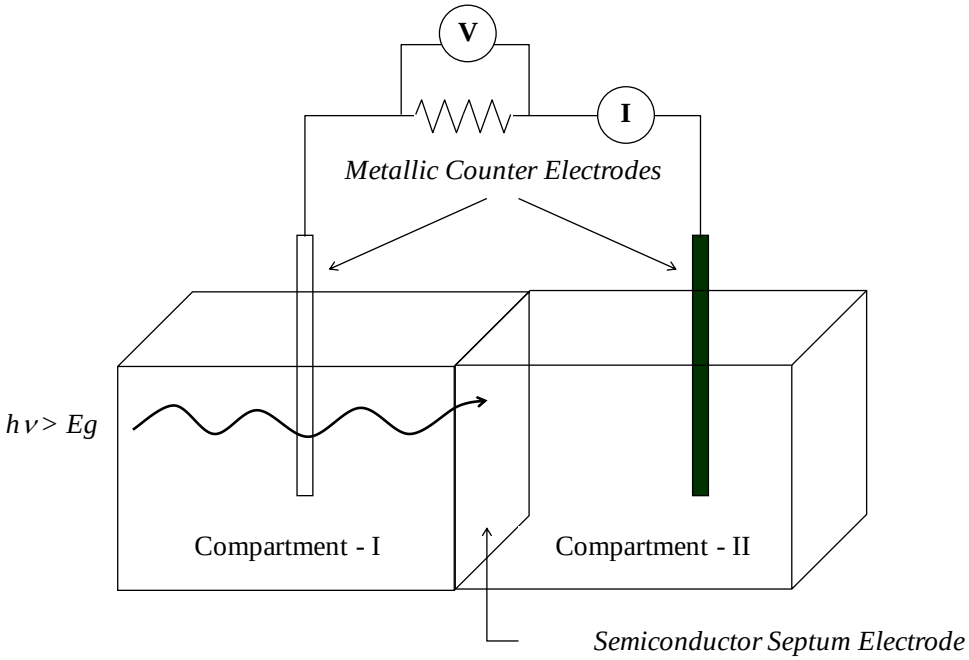

Fig.2.9- Schematic diagram of the semiconductor-septum storage cell

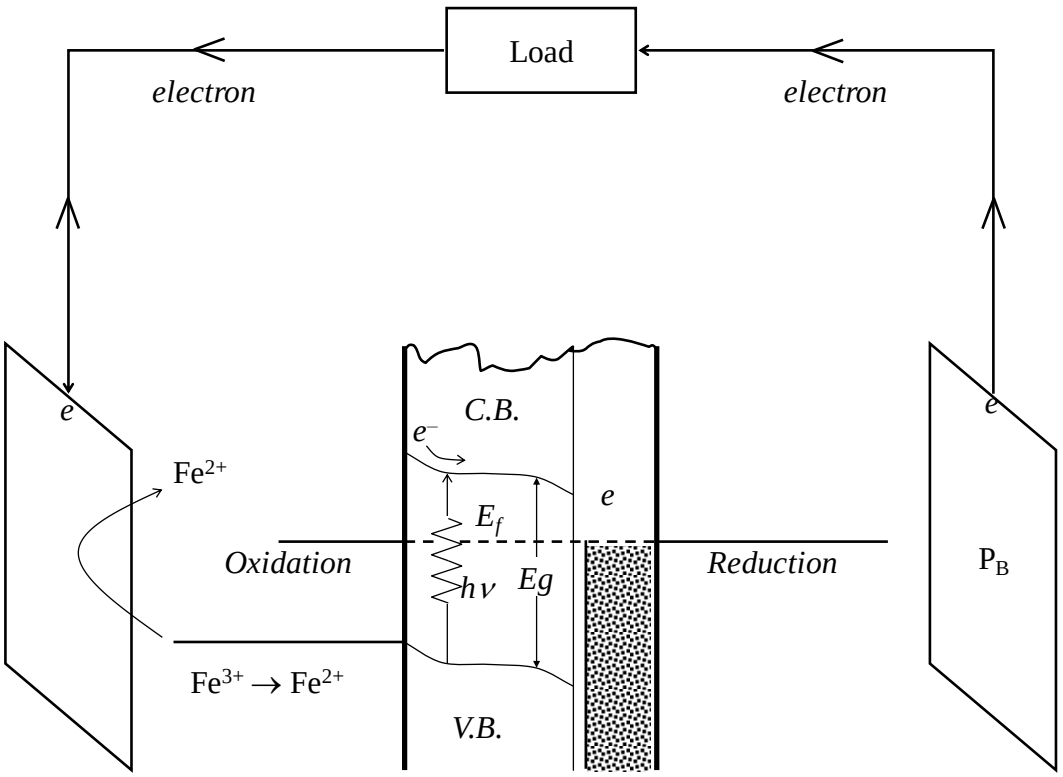

Fig.2.10 - The mechanism and operation of SC-SEP cell

The semiconductor septum cell under illumination causes generation of electron hole pairs, the electron jump into the conduction band from valence band. The electron further moves towards the bulk of the semiconductor and via metallic substrate travels into the other compartment where it is received by the oxidized species, and reduces the oxidized species. These oxidized species gets either reduced to lower oxidation state or to metal. These species can again be reoxidized by transferring an electron to the metal electrode in compartment II, in dark, while hole moves torwards the surface of the semiconductor and accepted by the reduced species present in compartment I and oxidises the reduced species. In dark, these oxidised species accept electrons from compartment II, resulted in the electricity flow through external load. The mechanism and operation of this SC-SEP cell is illustrated in Fig. 2.10.

For the Fe^{2+} and Fe^{3+} electrolytes in I compartments, the reactions are as follows

$$\text{Semiconductor} + h\nu \leftrightarrow e^{-}\ (\text{C.B.}) + h^{+}\ (\text{V.B.})$$

$$n\ Fe^{2+} + n\ h^{+} \leftrightarrow n\ Fe^{3+} \qquad \text{Compartment I}$$

$$n\ M^{n} + n\ e^{-} \leftrightarrow n\ M^{n-1} \qquad \text{Compartment II}$$

where ‘M’ denotes various redox species present in compartment II.

During charging these reaction shift from left to right and in the opposite direction during discharging. Thus, the system could be charged photoelectrochemically for the production of electricity upon demand.

However SC-SEP solar cell shows promise not only for generation of electricity but also for producing chemicals.

REFERENCES

1. K.L. Chopra, 'Thin Film Phenomena', McGraw Hill Book Co., New York, (1969).

2. H.P. Klug and H.E. Alexander, 'X-ray Diffraction Procedure', 2nd Edition, New York, Wiley, (1974).

3. L.Zwell and A.W.Danko, 'Applied Spectroscopy Reviews', 9 (1975) 167.

4. A.S.Charles, M. Nenadic and J. Crable, 'Developements in Applied Spectroscopy', 9 (1971) 343.

5. G.R. Pulliam, J.Appl. Phys., 38 (1967) 1120.

6. J. Jeorge and M.K. Radhakrishnan, Solid State Comm., 33 (1980) 987.

7. R.R. Helks and R.W. Ure, 'Thermoelectricity Sci. and Engineering', Instur. Sci. New York, (1961), Chapt.3.

8. F. Micheltti and P. Mark, J. Appl. Phys. (Lett.), 10 (1967) 136.

9. E. Becquerel, Comt. Rend. H.A., 9 (1839) 561.

10. M.D. Archer, J. Appl. Electrochem., 5 (1975) 17.

11. H. Gerischer, Pure and Appl. Chem., 52 (1980) 2449.

12. R. Parkinsons, J. Electrochem. Soc., 127 (1980) 1766.

13. J.O.M. Bockris and A.K.N. Reddy, 'Modern Electrochemestry', Vol.2, A Plenum, Rostta Edition, (1974) Chapt.- 7, p. 8.

14. D.R. Craw,'Principles of Applied Electrochemistry', Chapman and Hall, London, (1974).

15. J.F. Mc Cann and S.P.S. Bad, J. Electrochem. Soc., 129 (1982) 521.

16. A.S. Hakhamanan and C.V. Suryanarayana, Trans. SAEST, 18 (1983) 281.

17. H. Gerisher, in ‘Semiconductor Liquid Junction Solar Cells.’, Ed. A. Heller, The Electrochem. Soc. Inc., New York, (1977) Chapt.3, p.1.

18. A. Aruchamy, G. Aravamudan and G.V. Subba Rao, Bull. Mat. Sci., 4 (1982) 483.

19. S. Mureramanzi, H.T. Tien, Int. J. Ambient Energy, 7 (1980) 3.

20. H. Gerischer, Top. Appl. Phys., 31 (1979) 115.

21. R. Memming, Prog. Surf. Sci., 17 (1984) 7.

22. S.H. Pawar and P.S. Patil, Bull. Electrochem., 6 (1990) 618.

23. H.T. Tien, Nature, 227 (1970) 1232.

24. J.R. Bottom, and D.O. Hall, Ann. Rev. Energy, 4 (1979) 352.

25. G. Porter and M.D. Archer, Interdisc Sci. Rev., (1976) 119.

26. H.T. Tien and B. Karveley, in ‘Solar Power and Fules’ (Ed). J.R. Botton, New York. (1977), p 167.